Switching of Reverse Charge Transfers for a Rational Design of an OFF−ON Phosphorescent Chemodosimeter of Cyanide Anions

Jean-Luc Fillaut,* Huriye Akdas-Kilig, Edouard Dean, Camille Latouche, and Abdou Boucekkine*

Institut des Sciences Chimiques de Rennes, UMR 6226 CNRS-Université de Rennes 1, 35042 Rennes Cedex, France

Ⓢ *Supporting Information*

ABSTRACT: A rational approach to luminescence turn-on sensing of cyanide by a dicyanovinyl-substituted acetylide Pt(II) complex, which primarily relies on the nucleophilic addition reaction of cyanide anions to the α-position of the dicyanovinyl group, is described. The strategy used for the design of this cyanide-selective sensor takes advantage of a switch of charge transfer from ML'CT to MLCT/L'LCT in this acetylide Pt(II) sensor. As a result, this chromophore that exhibits almost no basal luminescence displays observable changes in its UV−visible spectrum and acquires strong phosphorescence upon addition of cyanide anions. DFT computations reveal that the frontier molecular orbitals of the anionic system obtained after addition of CN⁻ are drastically different from those of the neutral initial species. TD-DFT computations permitted a full assignment of the observed absorption bands and explained well the emissive properties of the species under consideration.
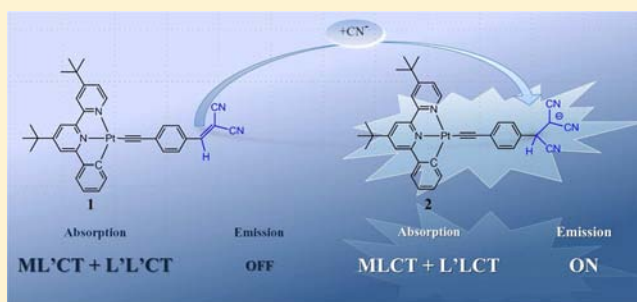
INTRODUCTION

Molecular recognition and sensing of anions is a major concern because of the roles that anions play in a wide range of biological, environmental, and chemical processes.[1−3] Thus, the development of sensitive anion luminescence sensors continues to be an important field of research.[4−8] In this field, transition metal complexes have attracted increasing interest due to their unique advantages that make them suitable for luminescent sensing.[8] The properties of the excited states are highly sensitive to the nature of the metal center, the type of ligands, and the local environment, allowing the photophysical properties (such as emission wavelength, lifetime, and intensity) of the metal complexes to be tailored for sensing applications.

Cyclometalated phenylbipyridyl complexes Pt(II) [Pt(tBu$_2$-C^N^N)(C≡C−R)][9−14] (tBu$_2$-C^N^N = 4,4′-di($tert$-butyl)-6-phenyl-2,2′-bipyridine), incorporating σ-alkynyl ligands, are characterized by high quantum efficiency and convenient absorption and emission maxima located in the visible spectrum with a large Stokes shift and relatively long lifetime ($\sim$1−20 μs). It is also noteworthy that the MLCT/LLCT transitions and ^{3}MLCT [Pt(5d) → π*(tBu$_2$-C^N^N)] emission are sensitive to electronic effects due to the substituents at the σ-alkynyl ligands.[13] Taking advantage of the properties of neutral cyclometalated polypyridyl Pt(II) complexes incorporating phenylacetylide ligands, it was previously demonstrated that the *para*-positions of the phenylacetylide group can be utilized as cation receptors, which are covalently bound to the cyclometalated Pt(II) signaling centers through Pt−acetylide σ-coordination.[10−12,14,15] The binding of cations to the receptors can induce optical signal switching between the

L'LCT (ligand-to-ligand charge transfer) and MLCT or ML'CT (metal-to-ligand charge transfer) excited states.[15] Such binding results in significant perturbation of the various photophysical properties of the Pt−acetylide complexes giving rise to changes in wavelengths, lifetimes, or quantum yields, which can be advantageous in the field of sensing.[8] Conversely, reports concerning anion recognition with alkynyl Pt(II) systems are rare.[16]

Here, we describe a new luminescence-enhanced anion sensing mechanism based on an inversion of metal-to-ligand and ligand-to-ligand charge transfers in a neutral cyclometalated phenylbipyridyl Pt(II) alkynyl complex[9,13,14] subsequent to the irreversible nucleophilic addition of a cyanide anion to the α-position of a dicyanovinyl group. The sensor was designed so that its luminescence is dramatically activated concomitantly with selective and sensitive responses to various concentrations of cyanide anion. Density functional theory (DFT) and time-dependent DFT (TD-DFT) calculations were carried out to help rationalize the observed properties.

EXPERIMENTAL SECTION

Synthesis: General Procedure. All manipulations were performed using Schlenk techniques under an Ar atmosphere. All commercially available starting materials were used as received. All solvents were dried and purified by standard procedures. The starting complex, [Pt(tBu$_2$-C^N^N)Cl], was prepared according to previously published methods.[13]

Physical Measurements and Instrumentation. NMR spectra were recorded on Bruker DPX-200, AV 300, or AV 500 MHz

Scheme 1
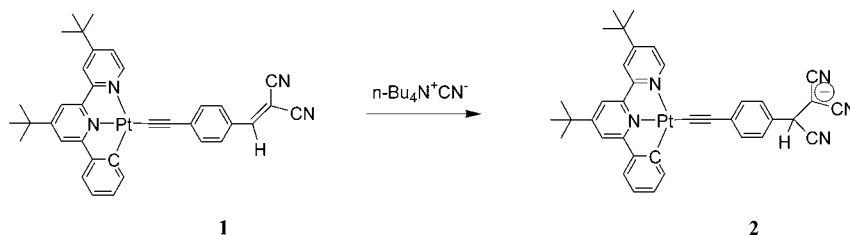
spectrometers. ^{1}H and ^{13}C chemical shifts are given versus SiMe$_4$ and were determined by reference to residual ^{1}H and ^{13}C solvent signals. High-resolution mass spectra (HRMS) were performed on a MS/MS ZABSpec TOF at the CRMPO (Centre de Mesures Physiques de l'Ouest) in Rennes. UV–vis absorption spectra were recorded using a UVIKON 9413 or Biotek Instruments XS spectrophotometer using quartz cuvettes of 1 cm path length.

Luminescence spectra were measured in dilute dichloromethane solutions ($\sim$10^{-6} M) using a FS920 steady-state fluorometer (Edinburgh Instruments). The spectra shown are corrected for the wavelength dependence of the detector, and the quoted emission maxima refer to the values after correction. Luminescence quantum yields were determined using the method of continuous dilution, using [Ru(bpy)$_3$]Cl$_2$ as the standard (Φ = 0.028 in air-equilibrated aqueous solution)^{17} and correcting for the refractive index.

Synthesis of 4. [Pt(tBu$_2$-C$^\wedge$N$^\wedge$N)Cl]^{13} (100 mg, 0.171 mmol) was added to a suspension of 4-(trimethylsilylethynyl)benzaldehyde^{18} (50 mg, 0.23 mmol), CuI (5.0 mg, 25 μmol), and K$_2$CO$_3$ (300 mg) in 20 mL of deoxygenated methanol and methylene chloride (1:1 v/v). The mixture was stirred at room temperature overnight. After evaporation of the solvents, the crude residue was purified by column chromatography on silica gel with dichloromethane/pentane/ethyl acetate (49/49/2) as eluent to give **4** as a yellow solid (60 mg, 52% yield). ^{1}H NMR (400 MHz; CDCl$_3$): 9.99 (s, 1H); 9.06 (dd, 1H, $^3J_{H-H}$ = 5.71 Hz, $^3J_{Pt-H}$ = 17.9 Hz); 7.88 (ddd, 1H, $^3J_{H-H}$ = 7.0 Hz, $^3J_{Pt-H}$ = 64 Hz, $^4J_{H-H}$ = 1.05 Hz); 7.81 (d, 1H, $^4J_{H-H}$ = 1.70 Hz); 7.80 (dd, $^3J_{H-H}$ = 7.42 Hz, $^5J_{H-H}$ = 1.26 Hz, 2H); 7.68 (dd, $^3J_{H-H}$ = 7.42 Hz, $^5J_{H-H}$ = 1.26 Hz, 2H); 7.58 (m, 2H); 7.51 (dd, 1H, $^3J_{H-H}$ = 7.90 Hz, $^4J_{H-H}$ = 1.27 Hz); 7.40 (dd, 1H, $^3J_{H-H}$ = 5.74 Hz, $^4J_{H-H}$ = 1.92 Hz); 7.17 (td, 1H, $^3J_{H-H}$ = 7.34 Hz, $^4J_{H-H}$ = 1.36 Hz); 7.08 (td, 1H, $^3J_{H-H}$ = 7.50 Hz, $^4J_{H-H}$ = 1.36 Hz); 1.47 (s, 9H); 1.45 (s, 9H). ^{13}C {^{1}H} NMR (75 MHz; CDCl$_3$): 191.4; 164.7; 164.2; 164.1; 158.1; 154.5; 151.3; 147.1; 142.1; 138.1; 135.8; 133.0; 132.1; 131.2; 129.8; 124.8; 124.2; 123.6; 119.3; 115.6; 115.2; 115.0; 106.5; 36.0; 35.7; 30.2; 30.0. m/z: 690.2061 ([M + Na]$^+$. C$_{33}$H$_{32}$N$_2$ONa^{195}Pt requires 690.2060). Elemental Anal. Found: C 59.30, H 5.09, N 3.88. Calcd for C$_{33}$H$_{32}$N$_2$OPt (667.33): C 59.34, H 4.83, N 4.20. Calcd for C$_{33}$H$_{32}$N$_2$OPt·0.5C$_4$H$_8$O$_2$ (711.355) (signals for ethylacetate were observed by ^{1}H NMR): C 59.04, H 5.10, N 3.94.

Synthesis of 1. [Pt(tBu$_2$-C$^\wedge$N$^\wedge$N)(4-C≡C−C$_6$H$_4$−CHO] (100 mg, 0.149 mmol) was added to a suspension of malononitrile (20 mg, 0.30 mmol) and basic alumina (100 mg) in 20 mL of deoxygenated toluene. After stirring at 60 °C overnight, the suspension was cooled to room temperature and filtered. Removal of the solvent in $vacuo$ and trituration of the solid residue by diethylether gave the desired product **1** as a reddish powder (95 mg, 84%). ^{1}H NMR (400 MHz; CD$_2$Cl$_2$): 8.97 (dd, 1H, $^3J_{H-H}$ = 5.75 Hz, $^3J_{Pt-H}$ = 17.9 Hz); 7.87 (ddd, 1H, $^3J_{H-H}$ = 6.95 Hz, $^3J_{Pt-H}$ = 64 Hz, $^4J_{H-H}$ = 1.07 Hz); 7.82 (d, 1H, $^4J_{H-H}$ = 1.72 Hz); 7.81 (d, 2H, $^3J_{H-H}$ = 7.78 Hz); 7.68 (s, 1H); 7.62 (s, 2H); 7.54 (m, 3H); 7.45 (dd, 1H, $^3J_{H-H}$ = 5.75 Hz, $^4J_{H-H}$ = 1.90 Hz); 7.11 (td, 1H, $^3J_{H-H}$ = 7.36 Hz, $^3J_{H-H}$ = 6.2 Hz, $^4J_{H-H}$ = 1.36 Hz); 7.07 (td, 1H, $^3J_{H-H}$ = 7.48 Hz, $^4J_{H-H}$ = 1.36 Hz); 1.47 (s, 9H); 1.45 (s, 9H). ^{13}C {^{1}H} NMR (75 MHz; CDCl$_3$): 165.2; 164.1; 163.9; 159.1; 158.1; 154.4; 151.6; 147.1; 141.7; 138.4; 136.8; 132.8; 132.7; 131.5; 131.0; 127.4; 124.7; 124.3; 123.9; 119.9; 119.3; 115.7; 114.8; 114.5; 113.6; 107.7; 78.8; 36.0; 35.8; 30.6; 30.4. m/z: 738.2170 ([M + Na]$^+$, C$_{36}$H$_{32}$N$_4$Na^{195}Pt requires 738.2167). Elemental Anal. Found: C

60.30, H 4.59, N 7.76. Calcd for C$_{36}$H$_{32}$N$_4$Pt (715.34): C 60.39, H 4.51, N 7.83.

Synthesis of 2. Compound **2** was prepared in $situ$ according to a general procedure: to the solution of **1** [Pt(tBu$_2$-C$^\wedge$N$^\wedge$N)(4-C≡C−C$_6$H$_4$−CH═C(CN)$_2$] (5 mg, 0.149 mmol) in 0.3 mL of CD$_2$Cl$_2$(CDCl$_3$) is added n-Bu$_4$NCN (1.9 mg, 0.149 mmol) in 0.3 mL CD$_2$Cl$_2$(CDCl$_3$). ^{1}H NMR (400 MHz; CD$_2$Cl$_2$): 9.07 (dd, 1H, $^3J_{H-H}$ = 5.73 Hz, $^3J_{Pt-H}$ = 17.8 Hz); 7.87 (d, 1H, $^4J_{H-H}$ = 1.72 Hz); 7.82 (ddd, 1H, $^3J_{H-H}$ = 6.95 Hz, $^3J_{Pt-H}$ = 64 Hz, $^4J_{H-H}$ = 1.07 Hz); 7.64−7.60 (m, 2H); 7.57 (dd, 1H, $^3J_{H-H}$ = 7.89 Hz, $^4J_{H-H}$ = 1.28 Hz); 7.40 (m, 3H); 7.42 (d, $^3J_{H-H}$ = 7.42 Hz, 1H); 7.34 (d, $^3J_{H-H}$ = 7.42 Hz, 1H); 7.13 (td, 1H, $^3J_{H-H}$ = 7.36 Hz, $^3J_{H-H}$ = 6.2 Hz, $^4J_{H-H}$ = 1.36 Hz); 7.08 (td, 1H, $^3J_{H-H}$ = 7.48 Hz, $^4J_{H-H}$ = 1.36 Hz); 4.27 (s, 1H); 1.47 (s, 9H); 1.45 (s, 9H). ^{13}C {^{1}H} NMR (75 MHz; CDCl$_3$): 165.2; 163.5; 163.4; 158.1; 154.5; 151.5; 147.1; 142.2; 138.5; 136.6; 133.6; 131.6; 130.9; 128.9; 124.5; 124.1; 123.5; 122.7; 121.3; 121.2; 119.1; 115.5; 114.4; 108.0; 105.1; 58.8; 37.2; 36.0; 35.7; 30.6; 30.4; 29.0; 19.7; 17.6; 13.6. The identity of the complex obtained was not able to be confirmed by mass spectrometry.

Computational Studies. Density functional theory (DFT) calculations were performed using the standard B3LYP functional$^{19−21}$ and a double-ζ LANL2DZ basis set,^{22} augmented with polarization functions on all atoms except hydrogen (exponents equal to 0.587 and 0.736, respectively, for the d functions of C and N and 0.8018 for the f function of Pt) with the Gaussian09^{23} program. At the very beginning of the computations, the geometries of complexes **1** and **2** in their singlet ground state were optimized. Solvent (CH$_2$Cl$_2$) effects have been taken into account using the PCM model.^{24,25} Then, the normal modes of vibration of the molecules were computed; all vibration frequencies were found to be real, confirming that the optimized geometries are minima on the potential energy surface. Finally, the computations of the ^{13}C NMR chemical shifts, as well as the electronic absorption spectra using time-dependent DFT (TD-DFT), were carried out at the same level of theory with the same Gaussian09 package, using the previously optimized ground-state geometries. In order to estimate the phosphorescence wavelengths, the relaxed triplet-state geometries of the complexes were obtained using both TD-DFT and unrestricted DFT computations. Drawings of molecular structures and orbitals were done using the Molekel program,^{26} while theoretical absorption spectra were plotted using Swizard,^{27} the half-bandwidths for the Gaussian model being taken equal to 2000 cm^{-1}. Percentage compositions of molecular orbitals (MOs) were analyzed using the AOMix program.^{28}

RESULTS AND DISCUSSION

Synthesis and Characterization. Our approach primarily relies on the nucleophilic addition reaction of cyanide to the dicyanovinyl-substituted acetylide Pt(II) complex **1** (Scheme 1). This dicyanovinyl-substituted Pt(II) chromophore exhibits almost no basal luminescence but acquires strong phosphorescence upon addition of cyanide anions.

The platinum(II) compound [Pt(tBu$_2$-C$^\wedge$N$^\wedge$N)(C≡C−C$_6$H$_4$−CH═C(CN)$_2$)] (tBu$_2$-C$^\wedge$N$^\wedge$N = 4,4′-di($tert$-butyl)-6-phenyl-2,2′-bipyridine), **1**, incorporating a dicyano-vinyl moiety was obtained in an overall yield of 30% in two steps from [Pt(tBu$_2$-C$^\wedge$N$^\wedge$N)Cl] as depicted in Scheme 2. The first step

Scheme 2
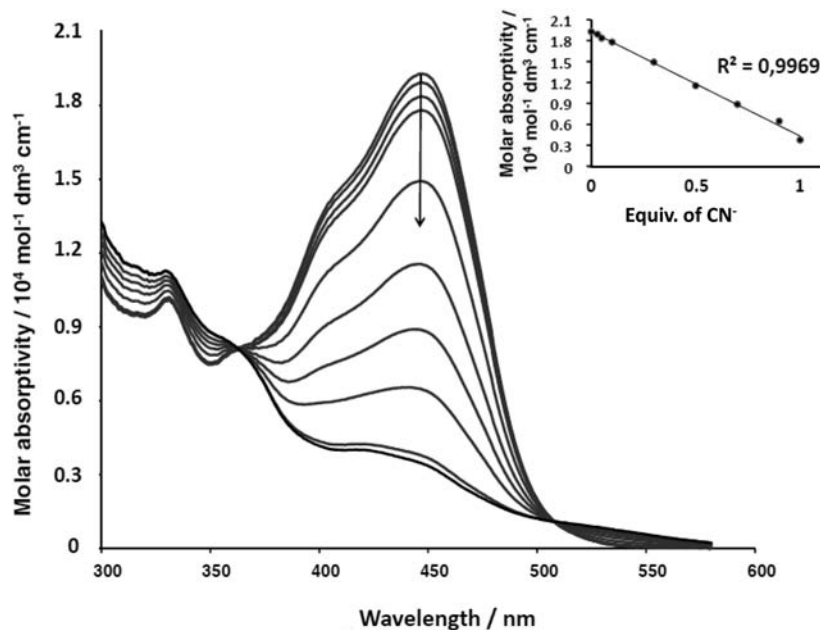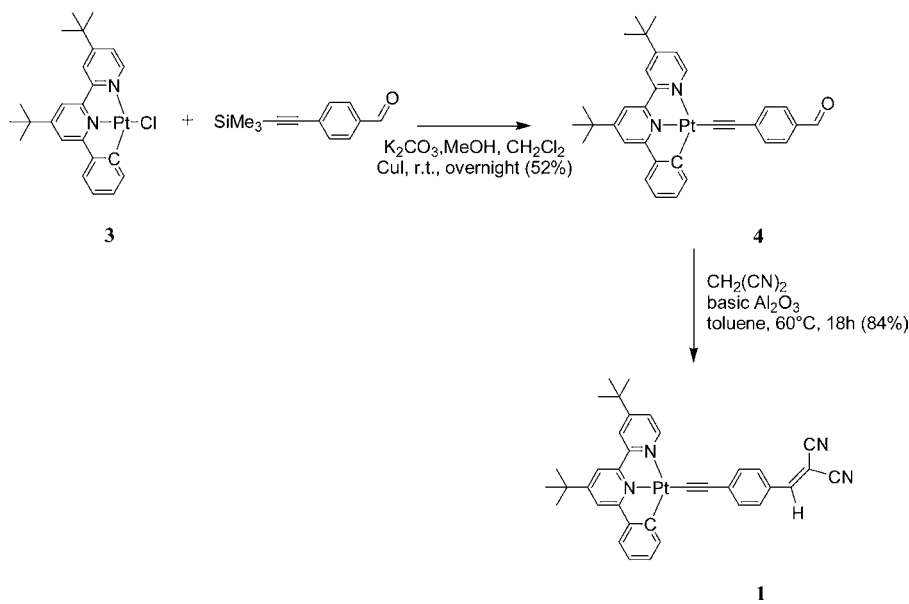
Figure 1. Changes in the UV−vis absorption spectrum of **1** (2.0×10^{-5} M in CH_2Cl_2) upon the addition of cyanide (($0-2.0$) $\times 10^{-5}$ M). Inset shows the absorption titration of **1** (2.0×10^{-5} M) at 450 nm with addition of n-Bu$_4$NCN in CH_2Cl_2 at 293 K. [n-Bu$_4$NCN] = (0, 0.06, 0.1, 0.2, 0.6, 0.8, 1.0, 1.2, 1.6, 2.0) $\times 10^{-5}$ M.

involves the one-pot reaction of 4-trimethylsilyl-ethynylbenzal-dehyde and [Pt(tBu$_2$-C^N^N)Cl] in presence of CuI (0.1 equiv) and an excess K$_2$CO$_3$ in CH$_3$OH−CH$_2$Cl$_2$ under anaerobic conditions. This step results in both the removal of the trimethylsilyl group and the coordination of the free alkyne to the [Pt(tBu$_2$-C^N^N)Cl] precursor. Finally, **1** was obtained by a Knoevenagel reaction of malononitrile in presence of basic alumina in toluene at 60 °C.

UV−Visible Absorption Spectroscopy. The UV−vis absorption characteristics of complex **1** strongly differ from the other [Pt(tBu$_2$-C^N^N)(C≡C−C$_6$H$_4$−R)] compounds.[9−15,29] The electronic absorption spectra of [Pt(tBu$_2$-C^N^N)(C≡C−C$_6$H$_4$−R)] exhibited intense absorption bands in the 330−360 nm range and less intense bands ($\varepsilon \approx$

5×10^3 dm^3 mol^{-1} cm^{-1}) in the 400−450 nm range. The broad low-energy bands in the 400−450 nm range were assigned as [dπ(Pt) → π^*(tBu$_2$-C^N^N)] MLCT transitions with mixing of some acetylide to diimine ligand [π(C≡C) → π^*(tBu$_2$-C^N^N)] ligand-to-ligand charge-transfer (L'LCT) transition. In contrast, complex **1** shows a very intense broad absorption band at 450 nm ($\varepsilon \approx 1.9 \times 10^4$ dm^3 mol^{-1} cm^{-1}) and a shoulder at 400 nm ($\varepsilon \approx 1.35 \times 10^4$ dm^3 mol^{-1} cm^{-1}). The strongest absorption band found at 450 nm was tentatively ascribed to ligand-centered (^{1}L'C) transitions, while the shoulder was assigned as a ML'CT (metal-to-ligand charge transfer to the alkynyl ligand).[12,15]

Not only does compound **1** display unusual absorption features, but excitation into these bands does not result in
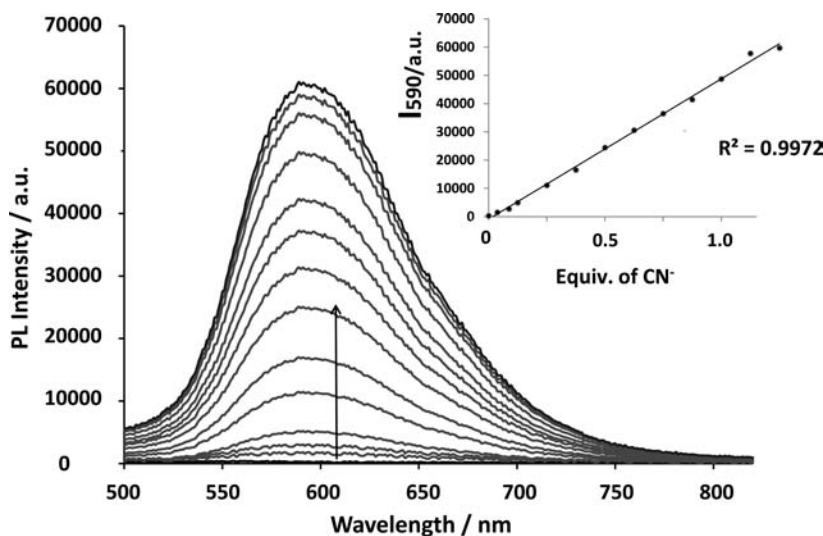
Figure 2. Changes in photoluminescence intensity of **1** (2.0×10^{-5} M in CH_2Cl_2) upon the addition of cyanide (($0-2.4) \times 10^{-5}$ M n-Bu$_4$NCN). Inset shows luminescence titration of **1** (2.0×10^{-5} M) with n-Bu$_4$NCN in CH_2Cl_2 at 293 K. [n-Bu$_4$NCN] = (0, 0.06, 0.1, 0.2, 0.3, 0.6, 0.8, 1.0, 1.2, 1.6, 2.0, 2.2, 2.4) $\times 10^{-5}$ M; λ_{ex} = 413 nm.

luminescence. We assume these characteristics to be caused by the presence of the dicyanovinyl fragment as a strong electron-withdrawing group (Hammett constant, σ_p = 0.84),[30] which makes the ML′CT transfer toward the electron-deficient ancillary acetylide ligand the lowest.[12,15]

Addition of Cyanide Anions. The cyanide anion is strongly nucleophilic; this property has been used advantageously in the design of fluorescent and colorimetric chemosensors.[7,31−37] Here, the nucleophilic addition reaction of cyanide to the α-position of the dicyanovinyl fragment was expected to result in the formation of the anionic species **2** (Scheme 1). This addition would not only reduce the extent of conjugation but also make the ancillary acetylide ligand less electron deficient. The anion binding affinity of **1** was thus evaluated by monitoring its UV−vis and steady-state emission properties as a function of anion concentration. Preliminary investigations revealed that the addition of cyanide anions, as tetra-n-butylammonium salts in CH_2Cl_2 to 2.0×10^{-5} M solutions of **1** caused significant changes to the UV−vis and steady-state emission properties. In control experiments, the addition of other anions (10 equiv of fluoride, chloride, dihydrogenphosphate, and acetate as tetra-n-butylammonium salts) did not have a marked effect on the absorption spectrum and emission of **1**. Finally, spectroscopic and luminescent responses of **1** toward hydroxyl ion (as tetramethylammonium hydroxide) as another strong nucleophile were studied. These control experiments clearly indicated that **1** does not respond to hydroxyl ion (see Figures S1 and S2, Supporting Information).

Figure 1 presents the changes in the UV−vis absorption spectrum of **1** as a function of CN$^-$ concentration. The low-lying ML′CT absorption and the ligand-based absorptions decrease monotonically throughout the addition with saturation observed toward the end of the titration. Two new broad low-energy bands (λ = 420 nm, $\varepsilon \approx 4.6 \times 10^3$ dm^3 mol^{-1} cm^{-1}; λ = 452 nm, $\varepsilon \approx 3.9 \times 10^3$ dm^3 mol^{-1} cm^{-1}) were assigned as the [dπ(Pt) → π*(tBu$_2$-C^N^N)] (MLCT) and [π(C≡C) → π*(tBu$_2$-C^N^N)] (L′LCT) charge-transfer transitions of complex **2**. The titration reaction curve of **1** toward the CN$^-$ ion was investigated as shown in Figure 1 (inset).

Concomitantly, the luminescent intensity (λ_{em} = 590 nm; λ_{ex} = 413 nm) is enhanced in response to the increase in the concentration of the added CN$^-$ ion in dichloromethane at room temperature (Figure 2). This emission (τ = 500 ns) may be due to emission from the ^{3}MLCT state related to the [Pt(tBu$_2$-C^N^N)(C≡C−C$_6$H$_4$−R)] acetylide system. To examine the sensitivity of **1** toward CN$^-$, its detection limit was evaluated. As shown in Figure 2 (inset), the emission titration profile of **1** (2.0×10^{-5} M) with CN$^-$ demonstrated that CN$^-$ could be detected at least down to 6×10^{-6} M, and the emission intensity of **1** increased linearly with the concentration of CN$^-$ (($0-2.0) \times 10^{-5}$ M) (R^2 = 0.9972).

To confirm the formation of the anionic species **2** (Scheme 2), the addition of cyanide anions was monitored by NMR. In the ^{1}H NMR (CD_2Cl_2) spectrum of **1** (Figure 3a), the dicyanovinylic CH proton signal is at 7.60 ppm. Upon addition of cyanide anions, 1.0 equiv, this signal disappeared, while a new singlet at 4.27 ppm was observed (Figure 3b). This singlet is consistent with the formation of a CH(CN)−C(CN)$_2^-$ fragment. In parallel, two doublets in the aromatic region at
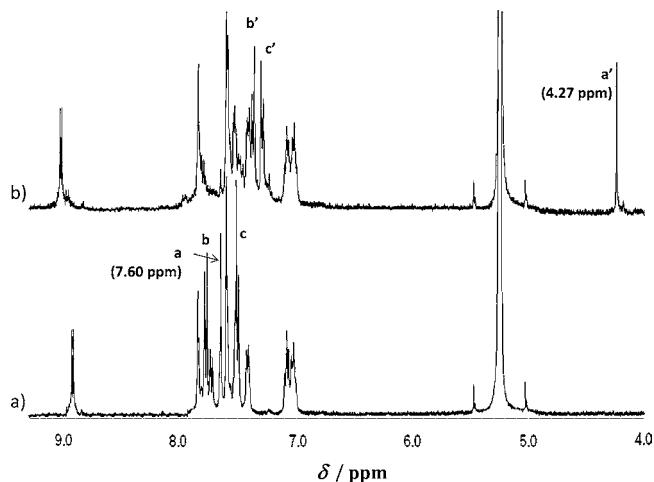
Figure 3. Partial ^{1}H NMR (CD_2Cl_2, 300 MHz) spectra of **1** (a) and that upon titration of 1 equiv of cyanide ions (as n-Bu$_4$N$^+$ salt) (b).

7.81 (b) and 7.54 ppm (c) are upfield shifted at 7.42 and 7.34 ppm (b′ and c′, respectively). These doublets were attributed to the aromatic protons of the phenylacetylide ligand, which are likely to be significantly affected upon addition of the cyanide anion to the dicyanovinyl moiety. On the other hand, the signals of the phenyl-bipyridine ligand were weakly affected. The hypothesis that the observed changes would be caused by the nucleophilic addition of cyanide is also supported by in situ ^{13}C NMR and DEPT experiments (CDCl$_3$): [13]C signals at 37.2 and 17.6 ppm in **2** can be tentatively attributed to the CH and C$^-$ carbon atoms of the CH(CN)−C$^-$(CN)$_2$ fragment, while the presence of three CN carbon atoms is confirmed (122.7, 121.3, and 121.2 ppm) (Figures S3 and S4, Supporting Information). DFT computations of the ^{1}H and ^{13}C chemical shifts fully confirm these assignments.

Computational Results. The computed ^{13}C NMR spectrum confirms the experimental assignments; in particular, the cyanovinylic carbon atom, C#29 (numbering of atoms and computed chemical shifts in Supporting Information) is found to experience a strong chemical shift from 71 ppm (carbon sp^2 hybridization, **1**) to 25 ppm (sp^3 hybridization, **2**), while C#28 is expected to shift from 171 (CH, sp^2 hybridization) to 46 ppm (CH, sp^3 hybridization), upon addition of CN$^-$. These values are in good agreement with the experimental ones (from 78.8 to 13.6 ppm for C#29 and from 159.1 to 58.8 ppm for C#28).

The frontier molecular orbitals (MOs) of complexes **1** and **2** are dramatically different (Figure 4). The highest occupied MOs
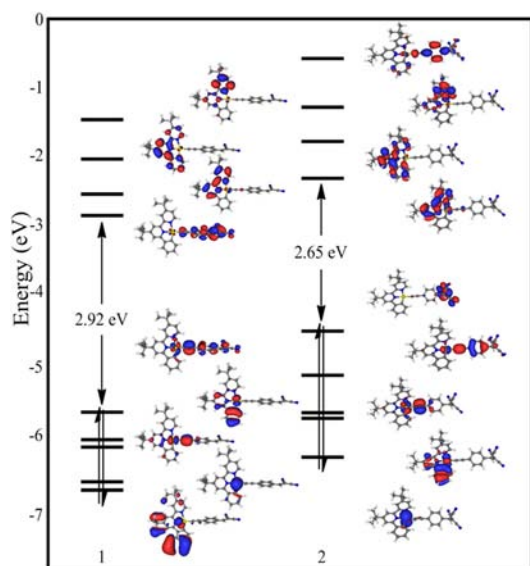
Figure 4. MO diagrams of **1** and **2**.

(HOMOs) of **1** are combinations of Pt(II) orbitals (15% (HOMO), 29% (HOMO − 1)) and L′ moiety orbitals (80% (HOMO), 52% (HOMO − 2)) or the phenyl-bipyridine ligand (5% (HOMO), 71% (HOMO − 1), 13% (HOMO − 2)); see Table 1 where the percentage weights of Pt, L, and L′ ligands in frontier MOs are given. Interestingly, the lowest unoccupied MO (LUMO) of complex **1** is mainly localized on the acetylide ligand L′. This is consistent with a strong stabilization of this LUMO due to the presence of the electron-

withdrawing dicyanovinylic unit.[15] Other LUMOs are mainly localized (about 93% (LUMO + 1) and 96% (LUMO + 2)) on the bipyridine part of the C^N^N moiety (ligand L).

The HOMO of **2** is fully localized on the H(CN)C−C(CN)$_2$ anionic moiety of the acetylide ligand L′ resulting from the addition of CN$^-$. This anionic moiety is clearly the strongest negative/electron-donating part of the complex. The other HOMOs of **2** are combinations of the Pt(II) orbitals (16% (HOMO − 1) and 28% (HOMO − 2)) and L′ moiety orbitals (79% (HOMO − 1) and 63% (HOMO − 2)). An almost pure d$_{z^2}$ orbital is present for both compounds in low-lying occupied frontier MOs (HOMO − 3 of **1** and HOMO − 4 of **2**). The latter MOs could be involved in high-energy excitations.

The LUMO, LUMO + 1, and LUMO + 2 of **2** are localized on the C^N^N ligand L. After addition of cyanide anions, the modified acetylide ligand cannot compete with the electron-withdrawing character of the bipyridine moiety: this leads to a drastic change of the electron distribution in the lowest unoccupied frontier MOs from **1** to **2** (Table 1).[38]

Table 2 provides the computed excitation energies, wavelengths, and oscillators strengths, as well as the λ_{max} of the bands of the simulated and experimental absorption spectra. The S$_0$ → S$_n$ excitations exhibiting a non-negligible oscillator strength are reported in this table. The corresponding electronic transitions and their weights in the excitations are given in the last column of the table. The calculated absorption spectra for **1** and **2** are displayed in Figure 5. A good agreement with the observed UV−visible absorption spectra of the two complexes is found, permitting a detailed assignment of the observed bands.

The simulated absorption spectrum of **1** exhibits an intense band at 467 nm and another one at 336 nm probably corresponding to the observed bands at 450 and 330 nm. Moreover, a very slight shoulder is present at 408 nm, which is likely to correspond to the experimental one at 400 nm. The highest computed wavelength of complex **1** at 467 nm (oscillator strength 1.37) corresponds to the HOMO → LUMO transition and is [1]L′L′CT/ML′CT in character (L′ = acetylide ligand; L = C^N^N). It can be also assigned as an intraligand (IL)/ML′CT transition. Computed transitions at 408 nm corresponding to conventional ML′CT/L′LCT transitions should contribute little to the absorption spectra because of their small oscillator strength (0.025). The second transition of significance (oscillator strength 0.25) at 336 nm is a mixed LLCT/MLCT from HOMO − 4, which has a slight metallic character.

For complex **2**, the calculations reveal a superposition of different types of excitations (IL, ligand−ligand charge transfer, MLCT) in the UV range. The lower energy excitations in the visible region appear at 529, 475, and 431 nm for **2**, leading to a large absorption band at λ_{max} roughly around 440 nm. These excitations do not lead to intense bands in the absorption spectra due to their small oscillator strengths. This is in line with the discoloration of the solution experimentally observed upon addition of cyanide anions (Figure 1). The computed bands at 475 and 431 nm (corresponding to the observed bands at 452 and 420 nm) involve several transitions from HOMO and HOMO − 1 to LUMO and LUMO + 1 and correspond to combined [π(C≡C) → π*(C^N^N)] ligand-to-ligand charge-transfer (L′LCT) and [dπ(Pt) → π*(C^N^N)] metal-to-ligand charge transfer (MLCT) transitions, while the computed transition at 529 nm (HOMO to LUMO) corresponds to a L′LCT transition with no metal character. It could correspond to the tail observed in the experimental spectra from 500 to 575 nm. A higher energy band is computed at 349 nm (330 nm experimentally) that involves several excitations, is more intense than the first ones, in agreement with experiment, and is a mix of MLCT/LLCT and L′LCT transitions.

Table 1. Percentage Weights of Pt/L/L′ in Frontier MOs

	H − 4	H − 3	H − 2	H − 1	H	L	L + 1	L + 2	L + 3
1	8/90/2	88/10/2	35/13/52	29/71/0	15/5/80	1/1/98	5/93/2	3/96/1	1/99/0
2	91/7/2	32/68/0	28/9/63	16/5/79	1/0/99	5/92/3	3/96/1	1/99/0	8/13/79

Table 2. TD-DFT Calculated Excitation Energies, Computed and Experimental Wavelengths and Weights of Transitions for Complexes 1 and 2

complex	energy, eV; λ, nm (oscillator strength)	excited states	λ_{max}, calcd [exp], nm	transitions (% weight)
1	2.66; 467 (1.3679)	$S_0 \rightarrow S_3$	467 [450]	H $\rightarrow$ L (+84%)
	3.04; 408 (0.0250)	$S_0 \rightarrow S_6$	[400]	H $-$ 3 $\rightarrow$ L (+56%); H $-$ 2 $\rightarrow$ L + 1 (38%)
	3.69; 336 (0.2540)	$S_0 \rightarrow S_{13}$	336 [330]	H $-$ 4 $\rightarrow$ L + 1 (+85%); H $-$ 2 $\rightarrow$ L + 2 (+9%)
2	2.34; 529 (0.0647)	$S_0 \rightarrow S_1$	440 [452] [420]	H $\rightarrow$ L (+89%); H $-$ 1 $\rightarrow$ L (+10%)
	2.61; 475 (0.0719)	$S_0 \rightarrow S_2$		H $-$ 1 $\rightarrow$ L (+86%); H $\rightarrow$ L (11%)
	2.88; 431 (0.0707)	$S_0 \rightarrow S_5$		H $\rightarrow$ L + 1 (+68%); H $-$ 3 $\rightarrow$ L (+25%)
	3.34; 371 (0.1266)	$S_0 \rightarrow S_8$	349 [330]	H $-$ 2 $\rightarrow$ L + 1 (+80%); H $-$ 3 $\rightarrow$ L + 1 (11%)
	3.41; 364 (0.0904)	$S_0 \rightarrow S_9$		H $-$ 3 $\rightarrow$ L + 1 (+85%); H $-$ 2 $\rightarrow$ L + 1 (+10%)
	3.67; 338 (0.2015)	$S_0 \rightarrow S_{13}$		H $-$ 5 $\rightarrow$ L (+87%); H $-$ 4 $\rightarrow$ L + 1 (6%)
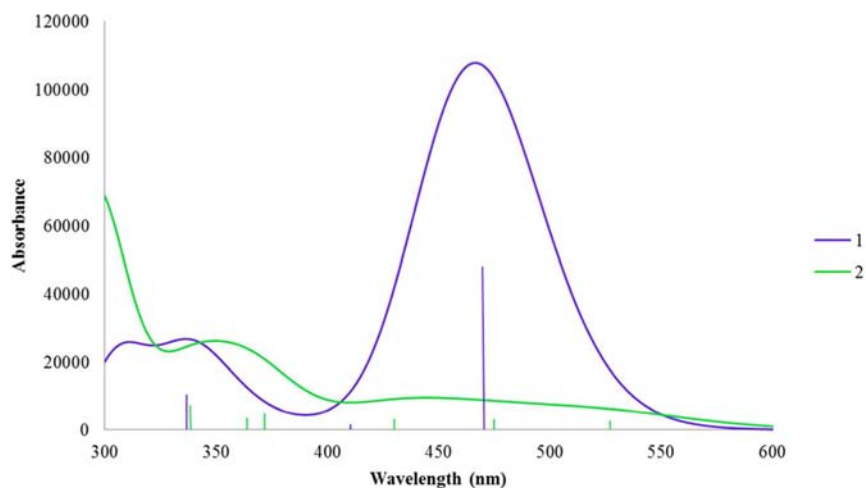
Figure 5. Computed absorption spectra of **1** and **2**.

Consequently, the observed changes in the absorption spectrum of **1** with addition of cyanide anions to **1** corresponds to a switch of charge transfers from L′L′CT/ML′CT in **1** (L′ = acetylide ligand) to L′LCT/MLCT in **2** (L = C^N^N). The HOMO → LUMO transition in **1** is mainly contributed from an electron excitation from the π orbital of the alkynyl ligand to the π* orbital of the alkynyl ligand leading to a nonemissive ligand-to-ligand charge-transfer excited state. The switch-on luminescent response to cyanide is attributed to the change in the lowest energy excited state of the system from this nonemissive ligand-to-ligand charge-transfer excited state to a phosphorescent metal-to-ligand charge-transfer excited state.

Using TD-DFT, we computed the phosphorescence wavelength from the triplet state arising from the above-mentioned transition of **2**. The obtained value (645 nm) is close to the experimental one (590 nm). These computed phosphorescence wavelengths correspond to emission from a triplet state with a main component HOMO − 1 to LUMO excited configuration, the LUMO being mainly localized on L for complex **2**. The nature of the lowest energy phosphorescence is thus attributed to a combination of ³L′LCT and ³MLCT transitions.[15]

The differences observed in the spin density plots obtained via unrestricted DFT computations of the T_1 triplet states (Figures S5 and S6, Supporting Information) of **1** and **2** agree with their contrasted emission properties. Indeed, a predominant localization of the spin density on the metal and on the L ligand of Pt(II) cyclometalated species is, in most cases, needed to warrant emission from the triplet states.[39,40] We observe first that the metal spin population in the T_1 state is slightly higher for the anionic species **2**, that is, 0.16 vs 0.11 for **1**. More significantly, the spin density plots show definitely different contributions of the alkynyl ligand L′ and of the cyclometalating ligand L for **1** and **2**: the sums of the atomic spin populations of ligand L are equal to 0.94 for the emissive species **2** and equal to 0.05 for the nonemissive species **1**, so that the unpaired spins are mainly localized on the L′ moiety for this last species and not on L. The T_1 state is thus

essentially L′L′CT in character with a small admixture of MLCT for **1**. By contrast, for **2**, the unpaired spins extend over a large spatial region of this anionic species, including the metal, the acetylide ligand L′, and particularly the bipyridine moiety of the L ligand, which is consistent with a luminescence due to combination of ³L′LCT and ³MLCT transitions.

Sensing Properties in a Water−Dichloromethane Biphasic System. Compound **1** has low solubility in water, which, in principle, could be advantageous in the development of an anionic sensing set based on a methylene chloride−water biphasic system. The rationale here is based on the fact that the 1:1 stoichiometric nucleophilic addition of cyanide to vinyl-substituted derivatives is irreversible and can be performed in aqueous medium.[35,41] It must be stressed that since an irreversible chemical reaction is used to produce the colorimetric response, compound **1** acts as cyanide-specific anion chemodosimeter[42−44] and will be subject to all the caveats that the use of a biphasic system implies (i.e., mass transfer limitations, fastness and intensity of response being potentially dependent on concentrations of both CN⁻ and **1**, and hydration of anions). Addition of tetra-*n*-butylammonium cyanide (10 equiv) to the aqueous phase of a methylene chloride−water biphasic system containing **1**, followed by stirring for several minutes, led to a partial discoloration in the organic phase that became slightly emissive ($\lambda_{em} \approx$ 590 nm; λ_{ex} = 413 nm) corresponding to the cyanide adduct **2**. Control experiments of the responses of **1** toward other anions did not lead to any detectable visual and spectral changes. Addition of NaCN (10 equiv in water) did not result in appreciable changes, but the subsequent addition of tetra-*n*-butylammonium chloride (10 equiv) to this aqueous phase, followed by

stirring for 2 min, resulted in the discoloration of the methylene chloride solution (see Figures S7 and S8, Supporting Information). These proof of concept experiments suggest that complexes such as **1** open up the possibility for producing novel phosphorescent chemodosimeters, with specific advantages. First, the off–on phosphorescent sensor **1/2** exhibits a significant Stokes shift (almost 150 nm, ~5800 cm^{-1}) for easy separation of excitation and emission. Second, its emission lifetime (τ = 500 ns) can easily discriminate signal from interference by fluorescent compounds. Finally, it shows high photostability and pH-independent emission (see Figure S9, Supporting Information) and open up the possibility of approaches to sensing based on the use of irreversible reactions.

CONCLUSION

In summary, this investigation has led to the development of a highly selective and sensitive chemodosimeter for detecting micromolar concentrations of CN$^-$ ions. Compound **1**, which serves as the basis of the detection system, reacts irreversibly with CN$^-$ in a 1:1 stoichiometric manner, a process that induces a large enhancement in the phosphorescence intensity. DFT and TD-DFT computations explain very well the switching of luminescence upon cyanide addition. Indeed, it has been shown that the frontier MOs that are involved in the absorption spectra of the neutral **1** and anionic **2** species are drastically different; only species **2** exhibits a MLCT/L′LCT excitation needed to ensure phosphorescence. Finally, the selectivity of this system for CN$^-$ over other anions is extremely high. The strategy for the sensor design presented here may thus contribute to the development of more efficient "Off–On" anion phosphorescent sensors.

ASSOCIATED CONTENT

Ⓢ Supporting Information

^{13}C NMR spectra (CDCl$_3$) of **1** and **2**, DFT optimized coordinates, optimized structures of **1** and **2**, most representative computed ^{13}C NMR chemical shifts, spin density plots of the triplet states, control experiments with other anionic salts, and tests of sensitivity to pH. This material is available free of charge via the Internet at http://pubs.acs.org.

AUTHOR INFORMATION

Corresponding Author

*E-mail: jean-luc.fillaut@univ-rennes1.fr (J.-L.F.), abdou.boucekkine@univ-rennes1.fr (A.B.).

Notes

The authors declare no competing financial interest.

ACKNOWLEDGMENTS

REFERENCES

(1) Gale, P. A. *Chem. Soc. Rev.* **2010**, *39*, 3746−3771.
(2) Gale, P. A. *Chem. Commun.* **2011**, *47*, 82−86.
(3) Gunnlaugsson, T.; Glynn, M.; Tocci, G. M.; Kruger, P. E.; Pfeffer, F. M. *Coord. Chem. Rev.* **2006**, *250*, 3094−3117.
(4) Duke, R. M.; Veale, E. B.; Pfeffer, F. M.; Kruger, P. E.; Gunnlaugsson, T. *Chem. Soc. Rev.* **2010**, *39*, 3936−3953.
(5) Galbraith, E.; James, T. D. *Chem. Soc. Rev.* **2010**, *39*, 3831−3842.
(6) Moragues, M. E.; Martínez-Máñez, R.; Sancenón, F. *Chem. Soc. Rev.* **2011**, *40*, 2593−2643.
(7) Yang, Y.; Zhao, Q.; Feng, W.; Li, F. *Chem. Rev.* **2013**, *113*, 192−270.
(8) Zhao, Q.; Li, F.; Huang, C. *Chem. Soc. Rev.* **2010**, *39*, 3007−3030.
(9) Clark, M. L.; Diring, S.; Retailleau, P.; McMillin, D. R.; Ziessel, R. *Chem.—Eur. J.* **2008**, *14*, 7168−7179.
(10) Lanoë, P.-H.; Fillaut, J.-L.; Guerchais, V.; Le Bozec, H.; Williams, J. A. G. *Eur. J. Inorg. Chem.* **2011**, *8*, 1255−1259.
(11) Lanoe, P.-H.; Fillaut, J.-L.; Toupet, L.; Williams, J. A. G.; Le Bozec, H.; Guerchais, V. *Chem. Commun.* **2008**, 4333−4335.
(12) Lanoë, P.-H.; Le Bozec, H.; Williams, J. A. G.; Fillaut, J.-L.; Guerchais, V. *Dalton Trans.* **2010**, *39*, 707−710.
(13) Lu, W.; Mi, B.-X.; Chan, M. C. W.; Hui, Z.; Che, C.-M.; Zhu, N.; Lee, S.-T. *J. Am. Chem. Soc.* **2004**, *126*, 4958−4971.
(14) Yang, Q. Z.; Wu, L. Z.; Zhang, H.; Chen, B.; Wu, Z. X.; Zhang, L. P.; Tung, C. H. *Inorg. Chem.* **2004**, *43*, 5195−5197.
(15) Latouche, C.; Lanoe, P.-H.; Williams, J. A. G.; Guerchais, V.; Boucekkine, A.; Fillaut, J.-L. *New J. Chem.* **2011**, *35*, 2196−2202.
(16) Fan, Y.; Zhu, Y.-M.; Dai, F.-R.; Zhang, L.-Y.; Chen, Z.-N. *Dalton Trans.* **2007**, 3885−3892.
(17) Nakamaru, K. *Bull. Chem. Soc. Jpn.* **1982**, *55*, 2697−2705.
(18) Fillaut, J.-L.; Perruchon, J.; Blanchard, P.; Roncali, J.; Golhen, S.; Allain, M.; Migalsaka-Zalas, A.; Kityk, I. V.; Sahraoui, B. *Organometallics* **2005**, *24*, 687−695.
(19) Lee, C.; Yang, W.; Parr, R. G. *Phys. Rev. B* **1988**, *37*, 785−789.
(20) Becke, A. D. *J. Chem. Phys.* **1993**, *98*, 5648−5652.
(21) Stephens, P. J.; Devlin, F. J.; Chabalowski, C. F.; Frisch, M. J. *J. Chem. Phys.* **1994**, *98*, 11623−11627.
(22) Hay, P. J.; Wadt, W. R. *J. Chem. Phys.* **1985**, *82*, 299−310.
(23) Frisch, M. J.; Trucks, G. W.; Schlegel, H. B.; Scuseria, G. E.; Robb, M. A.; Cheeseman, J. R.; Scalmani, G.; Barone, V.; Mennucci, B.; Petersson, G. A.; Nakatsuji, H.; Caricato, M.; Li, X.; Hratchian, H. P.; Izmaylov, A. F.; Bloino, J.; Zheng, G.; Sonnenberg, J. L.; Hada, M.; Ehara, M.; Toyota, K.; Fukuda, R.; Hasegawa, J.; Ishida, M.; Nakajima, T.; Honda, Y.; Kitao, O.; Nakai, H.; Vreven, T.; Montgomery, J. A., Jr.; Peralta, J. E.; Ogliaro, F.; Bearpark, M.; Heyd, J. J.; Brothers, E.; Kudin, K. N.; Staroverov, V. N.; Kobayashi, R.; Normand, J.; Raghavachari, K.; Rendell, A.; Burant, J. C.; Iyengar, S. S.; Tomasi, J.; Cossi, M.; Rega, N.; Millam, J. M.; Klene, M.; Knox, J. E.; Cross, J. B.; Bakken, V.; Adamo, C.; Jaramillo, J.; Gomperts, R.; Stratmann, R. E.; Yazyev, O.; Austin, A. J.; Cammi, R.; Pomelli, C.; Ochterski, J. W.; Martin, R. L.; Morokuma, K.; Zakrzewski, V. G.; Voth, G. A.; Salvador, P.; Dannenberg, J. J.; Dapprich, S.; Daniels, A. D.; Farkas, O.; Foresman, J. B.; Ortiz, J. V.; Cioslowski, J.; Fox, D. J. *Gaussian 09*, revision A.02; Gaussian, Inc.: Wallingford, CT, 2009.
(24) Cossi, M.; Scalmani, G.; Rega, N.; Barone, V. *J. Chem. Phys.* **2002**, *117*, 43−54.
(25) Barone, V.; Cossi, M.; Tomasi, J. *J. Chem. Phys.* **1997**, *107*, 3210−3221.
(26) Varetto, U. Molekel, version 5.4.0.8; Swiss National Supercomputing Centre: Lugano, Switzerland.
(27) Gorelsky, S. I. Swizard program, revision 4.5; http://www.sg-chem.net/swizard.
(28) Gorelsky, S. I. AOMix: Program for Molecular Orbital Analysis; University of Ottawa, http://www.sg-chem.net/aomix, 2009.
(29) Fillaut, J.-L.; Andriès, J.; Marwaha, R. D.; Lanoë, P.-H.; Lohio, O.; Toupet, L.; Williams, J. A. G. *J. Organomet. Chem.* **2008**, *693*, 228−234.
(30) Hansch, C.; Leo, A.; Taft, R. W. *Chem. Rev.* **1991**, *91*, 165−195.
(31) Ekmekci, Z.; Yilmaz, M. D.; Akkaya, E. U. *Org. Lett.* **2008**, *10*, 461−464.
(32) Kim, H. J.; Ko, K. C.; Lee, J. H.; Lee, J. Y.; Kim, J. S. *Chem. Commun.* **2011**, *47*, 2886−2888.
(33) Lee, K.-S.; Kim, H.-J.; Kim, G.-H.; Shin, I.; Hong, J.-I. *Org. Lett.* **2007**, *10*, 49−51.
(34) Liu, J.; Liu, Y.; Liu, Q.; Li, C.; Sun, L.; Li, F. *J. Am. Chem. Soc.* **2011**, *133*, 15276−15279.
(35) Liu, Z.; Wang, X.; Yang, Z.; He, W. *J. Org. Chem.* **2011**, *76*, 10286−10290.

(36) Xu, Z.; Chen, X.; Kim, H. N.; Yoon, J. *Chem. Soc. Rev.* **2010**, *39*, 127−137.

(37) Yang, Y.-K.; Tae, J. *Org. Lett.* **2006**, *8*, 5721−5723.

(38) Lee, C.-H.; Yoon, H.-J.; Shim, J.-S.; Jang, W.-D. *Chem.—Eur. J.* **2012**, *18*, 4513−4516.

(39) Yersin, H., Ed. *Transition Metal and Rare Earth Compounds*; Springer: Berlin, 2004; Vol. *241*, pp 1−26.

(40) Murphy, L.; Williams, J. A. G. In *Topics in Organometallic Chemistry*; Le Bozec, H., Guerchais, V., Eds.; Springer: Heidelberg, Germany, 2010; Vol. *28*; pp 75−111.

(41) Cheng, X.; Tang, R.; Jia, H.; Feng, J.; Qin, J.; Li, Z. *ACS Appl. Mater. Interfaces* **2012**, *4*, 4387−4392.

(42) Chae, M. Y.; Czarnik, A. W. *J. Am. Chem. Soc.* **1992**, *114*, 9704−9705.

(43) Kaur, K.; Saini, R.; Kumar, A.; Luxami, V.; Kaur, N.; Singh, P.; Kumar, S. *Coord. Chem. Rev.* **2012**, *256*, 1992−2028.

(44) Du, J.; Hu, M.; Fan, J.; Peng, X. *Chem. Soc. Rev.* **2012**, *41*, 4511−4535.